JOURNAL OF VIROLOGY, Oct. 2011, p. 10627–10638 Vol. 85, No. 20
0022-538X/11/$12.00 doi:10.1128/JVI.00757-11

Inhibition of Retromer Activity by Herpesvirus Saimiri Tip Leads to CD4 Downregulation and Efficient T Cell Transformation▽

Dior Kingston,[1,2]† Heesoon Chang,[1,3]† Armin Ensser,[4] Hye-Ra Lee,[1,3] Jongsoo Lee,[1,3] Sun-Hwa Lee,[3] Jae Ung Jung,[1,3]* and Nam-Hyuk Cho[1,5]*

Department of Microbiology and Molecular Genetics and Tumor Virology Division, New England Primate Research Center, Harvard Medical School, Southborough, Massachusetts 01772-9102[1]; Institute for Research in Biomedicine, Via Vincenzo Vela 6, 6500 Bellinzona, Switzerland[2]; Molecular Microbiology & Immunology, University of Southern California, School of Medicine, 2011 Zonal Avenue, HMR401, Los Angeles, California 90033[3]; Institut für Klinische und Molekulare Virologie, Friedrich-Alexander-Universität Erlangen-Nürnberg, D-91054 Erlangen, Germany[4]; and Department of Microbiology and Immunology, Seoul National University College of Medicine, and Institute of Endemic Disease, Seoul National University Medical Research Center and Bundang Hospital, Jongno-Gu, Seoul 110-799, Republic of Korea[5]

Received 14 April 2011/Accepted 8 August 2011

The mammalian retromer is an evolutionally conserved protein complex composed of a vacuolar protein sorting trimer (Vps 26/29/35) that participates in cargo recognition and a sorting nexin (SNX) dimer that binds to endosomal membranes. The retromer plays an important role in efficient retrograde transport for endosome-to-Golgi retrieval of the cation-independent mannose-6-phosphate receptor (CI-MPR), a receptor for lysosomal hydrolases, and other endosomal proteins. This ultimately contributes to the control of cell growth, cell adhesion, and cell migration. The herpesvirus saimiri (HVS) tyrosine kinase-interacting protein (Tip), required for the immortalization of primary T lymphocytes, targets cellular signaling molecules, including Lck tyrosine kinases and the p80 endosomal trafficking protein. Despite the pronounced effects of HVS Tip on T cell signal transduction, the details of its activity on T cell immortalization remain elusive. Here, we report that the amino-terminal conserved, glutamate-rich sequence of Tip specifically interacts with the retromer subunit Vps35 and that this interaction not only causes the redistribution of Vps35 from the early endosome to the lysosome but also drastically inhibits retromer activity, as measured by decreased levels of CI-MPR and lower activities of cellular lysosomal hydrolases. Physiologically, the inhibition of intracellular retromer activity by Tip is ultimately linked to the downregulation of CD4 surface expression and to the efficient *in vitro* immortalization of primary human T cells to interleukin-2 (IL-2)-independent permanent growth. Therefore, HVS Tip uniquely targets the retromer complex to impair the intracellular trafficking functions of infected cells, ultimately contributing to efficient T cell transformation.

The retromer complex is conserved from yeast to humans and is required for retrograde trafficking from the endosome to the trans-Golgi network (14, 20, 43–45). The most well-characterized receptor that requires retromer function is the cation-independent mannose-6-phosphate receptor (CI-MPR), which delivers newly synthesized mannose-6-phosphate-modified lysosomal hydrolases to the lysosome (2, 44, 48, 50). In humans, the retromer complex is comprised of five subunits. The Vps35 retromer subunit determines cargo specificity and acts as a scaffold through its interaction with Vps26 and Vps29, which leads to the stabilization of the core complex (11, 14, 20, 36, 37, 47). Sorting nexins 1 (SNX1) and 2 bind to Vps35 and facilitate the retromer complex's exit from the early endosomes through tubules, which occurs via self-assembly of the sorting nexins (7, 25, 29, 54). The same receptor can undergo multiple rounds of delivery, allowing for the recycling of CI-MPR. In addition to this role, the retromer complex also plays a critical role in the Wnt signaling pathway during the development of both *Caenorhabditis elegans* and *Drosophila* (12, 17, 41). Furthermore, in mammalian cells, retromer has been implicated in the transcytosis of the IgA receptor, and it has been suggested that retromer is involved in the trafficking of β-secretase protease, which is associated with the progression of Alzheimer's disease (21, 49, 52).

Herpesvirus saimiri (HVS) is apathogenic in its natural host, the squirrel monkey, but experimental HVS infection in rhesus macaques, common marmosets, and rabbits causes fulminant lymphoma and death (16). Only the HVS subgroup C can strongly immortalize primary T cells from both Old and New World monkeys, as well as human T cells, to cause interleukin-2 (IL-2)-independent, permanent growth. While Tip is not required for viral replication in culture, Tip expression is critical for T cell and Stp-C oncogene immortalization (13). Transformation of human T cells with recombinant HVS expressing a mutant Tip that is unable to bind Lck has shown that the Tip-Lck interaction is required for HVS-induced transformation of human T lymphocytes, while binding to STAT3 is not

* Corresponding author. Mailing address for Jae Ung Jung: Department of Molecular Microbiology and Immunology, University of Southern California, Keck Medical School, Harlyne J. Norris Cancer Research Tower, Room 5517, 1450 Biggy Street, Los Angeles, CA 90033. Phone: (323) 442-1713. Fax: (323) 442-1721. E-mail: jaeujung@usc.edu. Mailing address for Nam-Hyuk Cho: Department of Microbiology and Immunology, Seoul National University College of Medicine, Jongno-Gu, Seoul 110-799, Republic of Korea. Phone: 82-2-740-8392. Fax: 82-2-743-0881. E-mail: chonh@snu.ac.kr.

† Both authors contributed equally to the study.

▽ Published ahead of print on 17 August 2011.

necessary (22, 23). Tip also targets p80, a lysosomal protein that consists of an N-terminal WD repeat domain and a C-terminal coiled-coil domain. Interaction of Tip with p80 facilitates lysosomal vesicle formation and subsequent recruitment of Lck into the lysosome for degradation (9, 10, 38, 39). Consequently, Tip interactions with Lck and p80 result in the downregulation of T cell receptor (TCR) and CD4 surface expression. Remarkably, the two interactions are functionally and genetically separable: the N-terminal p80 interaction is responsible for TCR downregulation, and the C-terminal Lck interaction is responsible for CD4 downregulation (10). Recently, we also reported that the membrane-proximal amphipathic helix preceding Tip's transmembrane (TM) domain mediates lipid raft localization and membrane deformation (33). In turn, this motif directs Tip's lysosomal trafficking and selective TCR downregulation.

Despite extensive biochemical studies of Tip's effects on T cell signal transduction, the mechanisms by which Tip contributes to HVS-induced T cell transformation remain open for further elucidation. Given that Tip is required for the immortalization of T cells by HVS, we purified protein complexes using the amino-terminal conserved glutamic acid-rich region of Tip to find additional cellular binding partners that may contribute to the transforming potential of Tip. In this report, we show for the first time that HVS Tip interacts with the retromer complex by binding Vps35. Expression of Tip changes the localization of Vps35 and thereby inhibits retromer retrograde activity. As a result, Tip interaction with Vps35 inhibits forward trafficking of CD4 to the cell surface. Furthermore, recombinant HVSs containing a Tip Vps35-binding mutant were no longer able to immortalize primary human T cells to IL-2-independent growth. In this way, the HVS Tip protein has evolved elaborate mechanisms involving interactions with various host cell machineries to ultimately contribute to continuous growth of the infected T cells.

MATERIALS AND METHODS

Recombinant constructs. pCIneo *myc* epitope-tagged human Vps26, Vps29, Vps35, and SNX1 were kindly provided by Carol Haft at the National Institutes of Health. For the Tip Δ24 mutant, the first 24 amino acids (aa) of Tip were deleted. For the Tip E/Q mutant, glutamic acids at the amino acid positions 6, 7, 9, 12, 15, 17, 23, and 24 were mutated to glutamines by PCR mutagenesis. Tip and its mutants were cloned into pFJ and pBabe expression vectors with an amino-terminal AU1 epitope tag. Human CD4 and Lck were cloned into pFJ vectors. For TipN42-GST (glutathione *S*-transferase), the first 42 amino acids of Tip were cloned into the pEBG vector. Wild-type (wt) Vps35 and its deletion constructs were cloned into the p3XFLAG-CMV vector (Sigma-Aldrich).

Cell culture and reagents. Jurkat T cells and 293T cells were grown in RPMI 1640 and Dulbecco's modified Eagle's medium, respectively, with both supplemented with 10% fetal bovine serum (FBS) and 1% penicillin-streptomycin (Gibco-BRL; Invitrogen). Jurkat T cells stably expressing Tip and its mutants, Tip Δ24 and Tip E/Q, which were cloned into pBabe vectors, were selected and maintained in complete medium containing 5 μg/ml puromycin. Jurkat T cells were electroporated using a Bio-Rad electroporator at 250 V and 975 μF in RPMI 1640 supplemented with 10% FBS in the absence of antibiotics. 293T cells were transiently transfected using calcium phosphate (Clontech) or transfectin (Bio-Rad). All chemicals were purchased from Sigma-Aldrich unless otherwise noted. Antibodies used were as follows: for Western blotting, mouse anti-AU1, mouse anti-Flag, and mouse anti-myc (clone 9E10) antibodies (Covance), mouse anti-CD4 antibody (Novus Biologicals), mouse anti-Lck antibody, mouse anti-β-tubulin antibody, and secondary antibodies conjugated to horseradish peroxidase (Santa Cruz Biotechnology), phosphotyrosine mouse anti-4G10 antibody (Upstate), rabbit anti-Vps26, -Vps29, -Vps35, and -SNX1 antibodies (all obtained from the NIH), goat anti-Vps26, -Vps29, and -Vps35 antibodies, rabbit anti-SNX1 antibody (Abcam), and rabbit antibody against CI-MPR, kindly provided by Paul Luzio; for immunofluorescence assay, mouse anti-Flag and mouse anti-myc antibodies (Covance), rabbit anti-AU1 antibody (Bethyl Laboratories), mouse anti-EEA1, mouse anti-Lamp1, and mouse anti-Lamp2 antibodies (Pharmingen), mouse anti-myc antibody conjugated to Alexa 488 (Upstate), and secondary anti-mouse or anti-rabbit antibody conjugated to Alexa 488, Alexa 568, or Alexa 633 (Molecular Probes, Invitrogen); for flow cytometry, mouse anti-TCR antibody directly conjugated to fluorescein isothiocyanate, mouse anti-CD45 antibody conjugated to allophycocyanin, and mouse anti-CD4 antibody conjugated to phycoerythrin (Pharmingen).

Protein purification and protein identification by mass spectrometry. 293T cells were transiently transfected with GST or TipN42-GST. Lysates were prepared in 0.5% NP-40 lysis buffer (150 mM NaCl, 0.5% Nonidet P-40, and 50 mM HEPES buffer, pH 8.0), containing protease and phosphatase inhibitors (Roche). Glutathione-uniflow resin beads (Clontech) were used to pull down GST or TipN42-GST from precleared cell lysates. Pulldowns were separated by sodium dodecyl sulfate-polyacrylamide gel electrophoresis (SDS-PAGE). The purified proteins were visualized by silver staining (Invitrogen), and unique protein bands were cut out and sent to the Taplin Biological Mass Spectrometry (MS) facility at the Harvard Medical School (Boston, MA) for mass spectrometry analysis.

Immunoprecipitation and immunoblotting. Cell lysates were prepared as described above in 0.5% NP-40 or radioimmunoprecipitation assay (RIPA) buffer (50 mM Tris-HCl [pH 7.5], 150 mM NaCl, 1% NP-40, 0.5% sodium deoxycholate, 0.1% SDS). Immunoprecipitated proteins were resolved by SDS-PAGE, transferred to polyvinylidene difluoride (PVDF) membranes (Bio-Rad), blocked in 5% milk in Tris-buffered saline with 0.05% Tween 20, incubated with primary antibodies, and incubated with secondary antibodies conjugated to horseradish peroxidase. Immunoblot detection of proteins was visualized by an enhanced chemiluminescence system (Pierce). Membranes were stripped (2% SDS, 60 mM Tris [pH 6.8], and 0.01 M 2-mercaptoethanol, preheated to 55°C), rotated for 10 min at room temperature, washed, and then blocked before the addition of antibody.

Confocal microscopy. Stably transfected cells or 48-h-posttransfection cells were spun down in a cytospin centrifuge and prepared for immunofluorescence staining, followed by confocal microscopy visualization on a TCS SP laser-scanning microscope (Leica Microsystems) as previously described (10).

Measurement of lysosomal hydrolase enzyme activities. Equal numbers of Jurkat T cells stably expressing Tip or its mutants were collected, and lysates were prepared in an enzyme lysis buffer (300 mM NaCl, 1% Triton X-100, 50 mM Tris-HCl [pH 7.4]). Protein concentration in the cell lysate was quantified by Bradford assay (Bio-Rad) using bovine serum albumin (BSA) as a standard. Equal amounts of total protein were used to measure enzyme activity. β-Glucuronidase activity and acid phosphatase activity were measured using 2.5 mM 4-methylumbelliferyl-β-D-glucuronide hydrate and 1 mM 4-methylumbelliferyl phosphate (Sigma-Aldrich) as substrates, respectively, in 0.1 M sodium acetate (pH 4.5) and incubated at 37°C for 90 min in black 96-well, clear-bottom plates (BD Falcon). The reaction was stopped using 0.25 M glycine buffer (pH 10.3). Fluorescence was measured on a fluorimeter (Perkin Elmer) with an excitation wavelength of 355 nm, and fluorescence intensity was read at 460 nm. Data were plotted using Prism 4 software (GraphPad Software). Graphs for the relative activities of beta-glucuronidase and acid phosphate show means ± standard deviations (SD).

Flow cytometry. Cells (5×10^5) were washed in RPMI 1640 with 10% FBS and incubated with antibody for 30 min on ice. After being washed with ice-cold PBS, cells were fixed with 4% paraformaldehyde. Fluorescence cytometry was performed with a FACScan (Becton Dickinson Co.). Data were analyzed using CellQuest software (Becton Dickinson Co.).

Trypsin treatment and CD4 recovery on the cell surface. Jurkat T cells (1×10^6) stably expressing Tip or its mutants were pelleted, resuspended in prewarmed 0.05% trypsin (Gibco-BRL; Invitrogen), incubated at 37°C for 15 to 30 min, followed by the addition of 100% FBS, and then spun down. Pellets were then incubated for the indicated periods in RPMI 1640 supplemented with 10% FBS. After each incubation period, cells were prepared for flow cytometry and fixed.

RNA isolation and qPCR. Total cellular RNAs were extracted with TRI reagent (Sigma) according to the manufacturer's instructions. One microgram of total RNA was treated by DNase I (Sigma) and reverse transcribed by the iScript cDNA synthesis kit (Bio-Rad), and the cDNAs were measured by quantitative real-time PCR (qPCR). The relative quantification of CD4 gene expression (forward primer, 5′-CTGGCTCTGGAAACCTCAC-3′: reverse primer, 5′-ACCCACACCGCCTTCTCC-3′) was calculated with the ΔΔ*CT* method, where 18S rRNA (forward primer, 5′-TTCGAACGTCTGCCCTATCAA-3′; reverse primer, 5′-GATGTGGTAGCCGTTTCTCAGG-3′) was used for normalization. qPCR was performed by using iQ SYBR green Supermix (Bio-Rad) and a

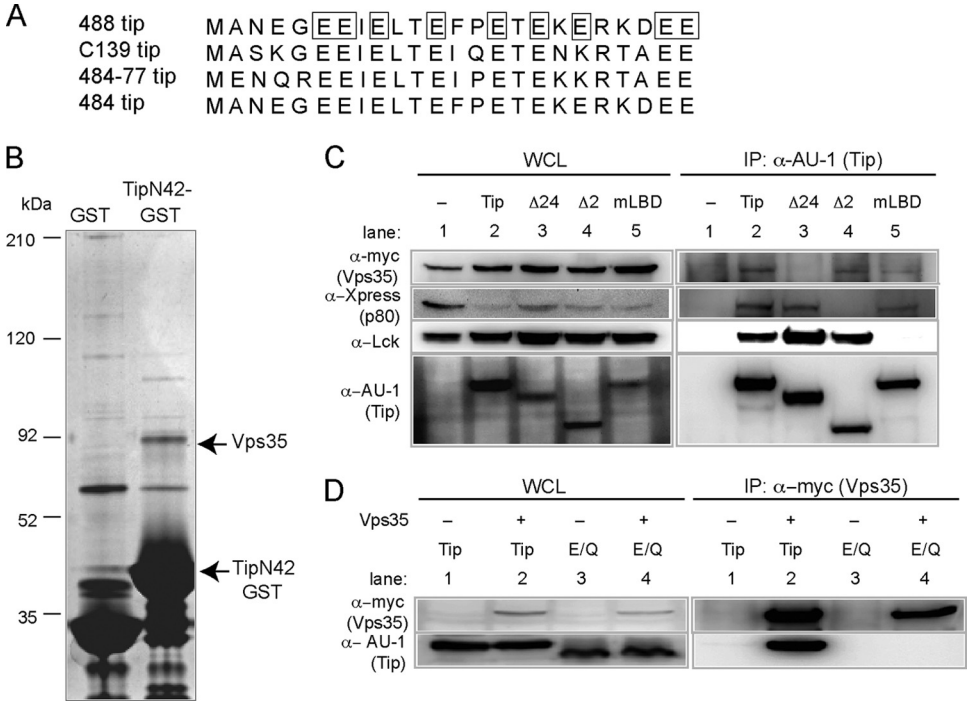

FIG. 1. Vps35 interacts with the amino-terminal glutamic acid-rich domain of Tip. (A) Amino acid sequence alignment of the first 24 amino acids of Tip isolates of various HVS subgroup C strains. Glutamic acid residues that were changed to glutamine in the Tip E/Q mutant are boxed. (B) Silver-stained SDS-PAGE from protein purification of GST and TipN42-GST. The 90-kDa band was identified as Vps35. (C) AU1-tagged Tip was immunoprecipitated (IP) from transfected 293T cells expressing *myc*-tagged Vps35, Xpress-tagged p80, and Lck, followed by Western blot analysis for interacting proteins. Numbers for whole-cell lysates (WCL) and IP correspond to the same conditions. Lane 1, vector; lane 2, wt Tip; lane 3, Tip Δ24 mutant; lane 4, Tip Δ2 mutant; and lane 5, Tip mLBD. (D) Immunoprecipitation of *myc*-tagged Vps35 in the presence of AU1-Tip (lanes 1 and 2) or AU1-Tip E/Q (lanes 3 and 4) from transfected 293T cells. Numbers for WCL and IP correspond to the same conditions. Control lanes 1 and 3 were not transfected with Vps35 (denoted by minus signs).

CFX96 real-time PCR machine (Bio-Rad). The PCR program was as follows: after an initial preincubation step at 95°C for 3 min, there were 40 cycles, each consisting of 95°C for 10 s, 59°C for 20 s, and 72°C for 20 s. The last amplification cycle was followed by a melt curve analysis to make sure about the specificity of the qPCR amplification.

Generation of recombinant virus production and verification of viruses. Recombinant viruses containing the described Tip E/Q or Tip 3Δ24 (deletion of amino acids 4 to 24) mutations were generated in cos331 as previously described (23). Recombinant viruses were obtained by transfecting 90% confluent owl monkey kidney (OMK) cells with Lipofectamine (Invitrogen) with equal amounts of each of the following cosmid backbones, cos261, cos290, cos336, cosDc5, and cos331, encoding wt Tip or the Tip E/Q or Tip 3Δ24 mutants. Supernatants containing the virus were collected from spreading infections after centrifugation. In order to verify the identity and purity of each recombinant virus, 2 μl of viral supernatants was subjected to PCR analysis with specific primers to amplify cosmid overlap regions as previously described (53), and titers (PFU) of recombinant viruses were determined by limiting dilutions (53).

Lymphocyte transformation and immortalization assays. Peripheral blood mononuclear cells from the blood of healthy donors were obtained after Ficoll gradient centrifugation. Cells were maintained in RPMI 1640 with 20% FBS. One million cells in 1 ml medium were infected with 100 μl ($\sim 5 \times 10^6$ PFU) of freshly isolated viral supernatant. Transformation was defined as aggregation and proliferation of cells for up to 3 months. Immortalization assays were performed by splitting the initial transformed cultures into two, and they were incubated with or without the addition of 10% IL-2 for two additional months. Transformation and immortalization were assessed by microscopically monitoring the cultures.

RESULTS

Interaction of Vps35 with the amino-terminal conserved region of Tip. Previous studies have shown that Tip interacts with multiple cellular proteins, such as Lck, STAT3, and p80, but only Lck has been shown to be required for transformation of HVS-infected T cells (4, 9, 22, 31, 39). To search for additional cellular Tip interaction partners that may contribute to *in vitro* T cell immortalization, the amino acid sequences of Tip proteins in various HVS subgroup C strains were analyzed, and a conserved glutamic acid-rich region at the amino terminus was discovered (Fig. 1A). Since this region was conserved among the different Tip isolates, we hypothesized that it may contribute to Tip function. Therefore, the first 42 amino acids of Tip, called TipN42, were fused to the amino terminus of GST for large-scale protein purification from 293T cells. Silver staining after SDS-PAGE showed a distinct band at 90 kDa in the lane expressing the TipN42-GST fusion protein but not in the GST control lane (Fig. 1B). Mass spectrometry analysis of this band identified peptides corresponding to the retromer subunit, Vps35.

In order to detect the Tip and Vps35 interaction, 293T cells were transfected with AU1-tagged wt Tip or Tip-binding mutants with *myc*-tagged Vps35 and used for immunoprecipitation with anti-AU1 antibody, followed by immunoblotting with the appropriate antibodies (Fig. 1C). Xpress-tagged p80 and Lck were included in a coimmunoprecipitation assay as controls. In the absence of Tip expression, none of these cellular proteins were detected in the anti-AU1 antibody immunoprecipitates. Upon wt Tip expression, all three proteins were ef-

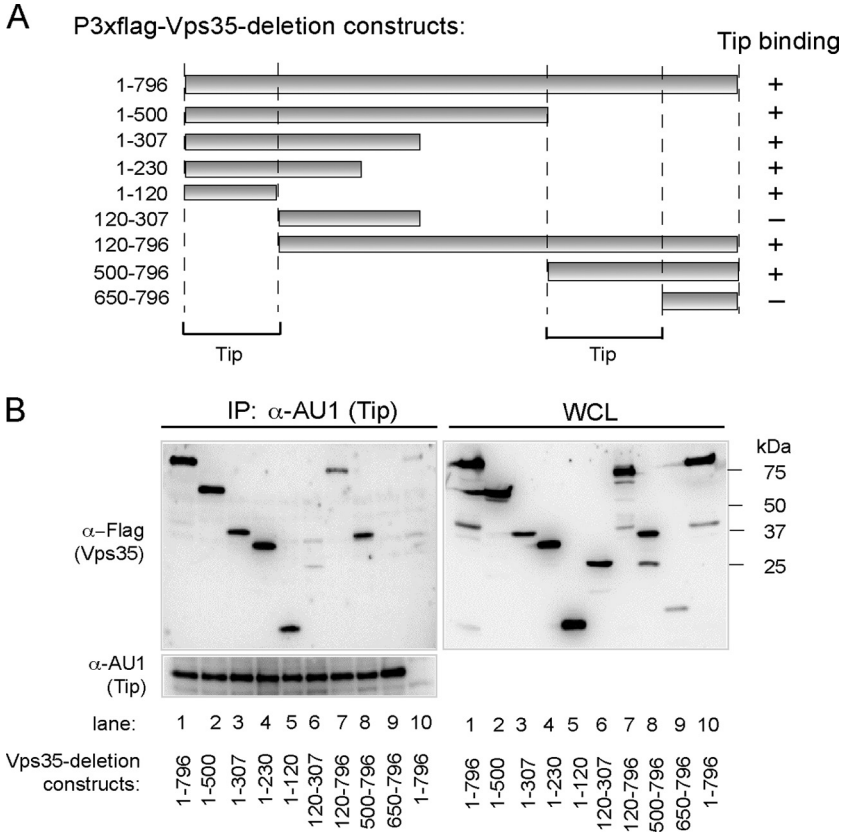

FIG. 2. Tip binds to amino acids 1 to 120 and 500 to 650 of Vps35. (A) Schematic diagram of Flag-tagged Vps35 deletion mutants used in binding assays. The plus and minus signs indicate binding and no binding, respectively, and the lines below the figures indicate the Tip-binding domains of Vps35. (B) Retromer binding activity of Tip mutants. At 48 h posttransfection with AU1-Tip wt and Flag-Vps35 wt or its deletion mutants, 293T cells were used for immunoprecipitation with anti-AU1 antibody, followed by Western blot analysis with anti-AU1 (Tip) or anti-Flag (Vps35) antibody. Lanes 1 to 9 express wt Tip, while lane 10 expresses only the vector. Vps35 construct expression was as follows: lanes 1 and 10, aa 1 to 796; lane 2, aa 1 to 500; lane 3, aa 1 to 307; lane 4, aa 1 to 230; lane 5, aa 1 to 120; lane 6, aa 120 to 307; lane 7, aa 120 to 796; lane 8, aa 500 to 796; and lane 9, aa 650 to 796.

ficiently coimmunoprecipitated (Fig. 1C, lane 2). A Tip mutant with the first 24 amino acids deleted (Tip Δ24 mutant) no longer interacted with Vps35 but was still bound to p80 and Lck (Fig. 1C, lane 3). As previously described (39), the Tip mutant with a deletion of amino acids 44 to 116, the Tip Δ2 mutant, no longer interacted with p80, but it still retained its interaction with Vps35 and Lck (Fig. 1C, lane 4). As expected, when the Tip mLBD mutant, with both the C-terminal Src-related kinase homology (CSKH) and Src homology 3 (SH3) motifs of the Lck-binding domain, was specifically point mutated, it lost its binding ability to Lck but was still able to bind to Vps35 and p80 (Fig. 1C, lane 5). In summary, the Vps35-binding region of Tip is located within its first 24 amino acids, and thus Tip interaction with Vps35 is genetically separable from its interactions with Lck and p80.

Given that the glutamic acid-rich sequence of Tip lies within the first 24 amino acids and is highly conserved among various isolates, each glutamic acid was changed to glutamine to generate the Tip E/Q mutant. While wt Tip efficiently bound to Vps35, the Tip E/Q mutant lost Vps35-binding ability (Fig. 1D, lane 4), indicating that the highly conserved glutamic acid-rich motif of Tip is required for its interaction with Vps35.

Tip binds to two separate regions of Vps35. To determine the Tip-binding regions of Vps35, the N- or C-terminal deletion constructs of Vps35 were fused to the N-terminal Flag epitope (Fig. 2A). The AU1tagged wt Tip was coexpressed with wt Vps35 or its deletion mutants, followed by immunoprecipitation and immunoblotting analysis. Vps35 wt 1–796 (numbers indicate amino acid positions) and the Vps35 1–500, 1–307, 1–230, 1–120, 120–796, and 500–796 mutants efficiently bound Tip, whereas the Vps35 120–307 and 650–796 mutants did not (Fig. 2A and B), suggesting that at least two domains of Vps35, amino acids 1 to 120 and 500 to 796, are independently capable of interacting with Tip. As controls for the integrity of the Vps35 deletion mutants, Vps26 and SNX1 were tested for their ability to bind to wt Vps35 or its mutants. These results show that Vps26 binds to the Vps35 1–796, 1–500, 1–307, and 1–230 proteins, while SNX1 binds to the Vps35 1–796, 1–500, 1–307, 1–230, 120–796, and 500–796 proteins and weakly to the 1–120 and 120–307 mutants (Fig. 3). These results agree with the previously published studies of yeast two-hybrid binding to the Vps26- and SNX1-binding domains (20). Thus, mutation analysis reveals two independent regions (aa 1 to 120 and 500 to 796) of Vps35 for Tip binding but also further provides evidence of a specific interaction between Vps35 and Tip.

Tip expression redirects Vps35 to lysosomal compartments. Retromer has been shown to localize primarily in the early

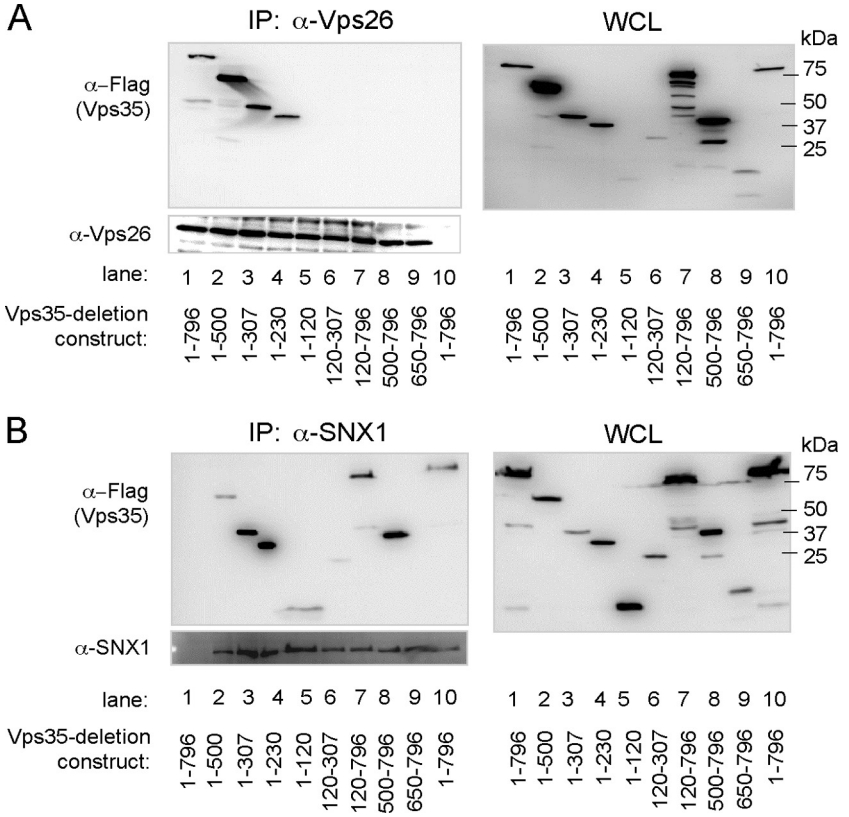

FIG. 3. Binding domains of Vps26 and SNX1 on Vps35. Vps35-binding activity of Vps26 (A) and SNX1 (B). At 48 h posttransfection with vectors expressing Vps26 or SNX1 and Flag-Vps35 wt or its deletion mutants, transfected 293T cell lysates were used for immunoprecipitation with anti-Vps26 or anti-SNX1 antibody, followed by Western blot analysis with anti-Vps26 or anti-SNX1 and anti-Flag (Vps35) antibodies. (A) Lanes 1 to 9 express Vps26, while lane 10 expresses only the vector. Vps35 construct expression was as follows: lanes 1 and 10, aa 1 to 796; lane 2, aa 1 to 500; lane 3, aa 1 to 307; lane 4, aa 1 to 230; lane 5, aa 1 to 120; lane 6, aa 120 to 307; lane 7, aa 120 to 796; lane 8, aa 500 to 796; and lane 9, aa 650 to 796. (B) Lane 1 expresses only the vector, while lanes 2 to 10 express SNX1. Vps35 construct expression was as follows: lanes 1 and 10, aa 1 to 796; lane 2, aa 1 to 500; lane 3, aa 1 to 307; lane 4, aa 1 to 230; lane 5, aa 1 to 120; lane 6, aa 120 to 307; lane 7, aa 120 to 796; lane 8, aa 500 to 796; and lane 9, aa 650 to 796.

endosomes of HeLa cells (2, 44). Immunofluorescence analysis also showed that Vps35 colocalized predominantly with EEA1 in Jurkat T cells but overlapped very little with either Lamp1 (Fig. 4A) or Lamp2 (data not shown), suggesting that Vps35 localizes in the early endosomes of Jurkat T cells. To demonstrate the effects of Tip interaction on Vps35 localization, the AU1-tagged Tip or its mutants and Flag-tagged Vps35 were electroporated into Jurkat T cells. They were then subjected to immunofluorescence staining with various antibodies 48 h postelectroporation. In addition to its apparent colocalization with Vps35, Tip induced the redistribution of Vps35 from small, punctate structures to large aggregates (Fig. 4B, top row). In contrast, the Tip Δ24 mutant or the nonbinding Tip E/Q mutant showed little or no colocalization with Vps35, nor did they induce large aggregated Vps35 structures (Fig. 4B, second and third rows). Surprisingly, upon Tip expression, Vps35 was apparently located in the Lamp2-containing lysosomal compartments as large aggregates rather than in the EEA1-containing early endosomal compartments (Fig. 4C). In contrast, upon Tip E/Q expression, Vps35 was predominantly located in the EEA-containing early endosomes with small, dispersed cytoplasmic staining (Fig. 4D). These results indicate that Tip expression induces the redistribution of Vps35 to lysosomal compartments, where both colocalize as large aggregates.

Tip deregulates retromer function. Given that Vps35 localization and lysosomal compartments are dramatically altered in Tip-expressing cells, retromer activity was tested in Jurkat T cell lines stably expressing Tip or its mutants by measuring the levels of CI-MPR, the most well-characterized cargo molecule of retromer action. Confocal microscopy analysis showed that CI-MPR staining levels were drastically reduced in wt Tip-expressing Jurkat T cells compared to those in vector-containing Jurkat T cells, while the levels were unaffected in Tip Δ24- or Tip E/Q-expressing Jurkat T cells (Fig. 5A). Immunoblotting analysis further confirmed these results, showing a marked reduction of CI-MPR levels upon wt Tip expression but not upon Tip Δ24 or Tip E/Q mutant expression (Fig. 5B). Furthermore, the Tip Δ2 mutant, which no longer bound p80 but retained Vps35 binding, and Tip mSH3B, which no longer bound Lck due to a mutation in the SH3-binding domain, also reduced CI-MPR levels as efficiently as wt Tip (Fig. 5B).

When enzymatic activity of the CI-MPR-dependent lysosomal hydrolase, β-glucuronidase, was measured, it was on average 3-fold lower in wt Tip-expressing Jurkat T cells than in vector-, Tip Δ24-, or Tip E/Q-expressing Jurkat T cells (Fig.

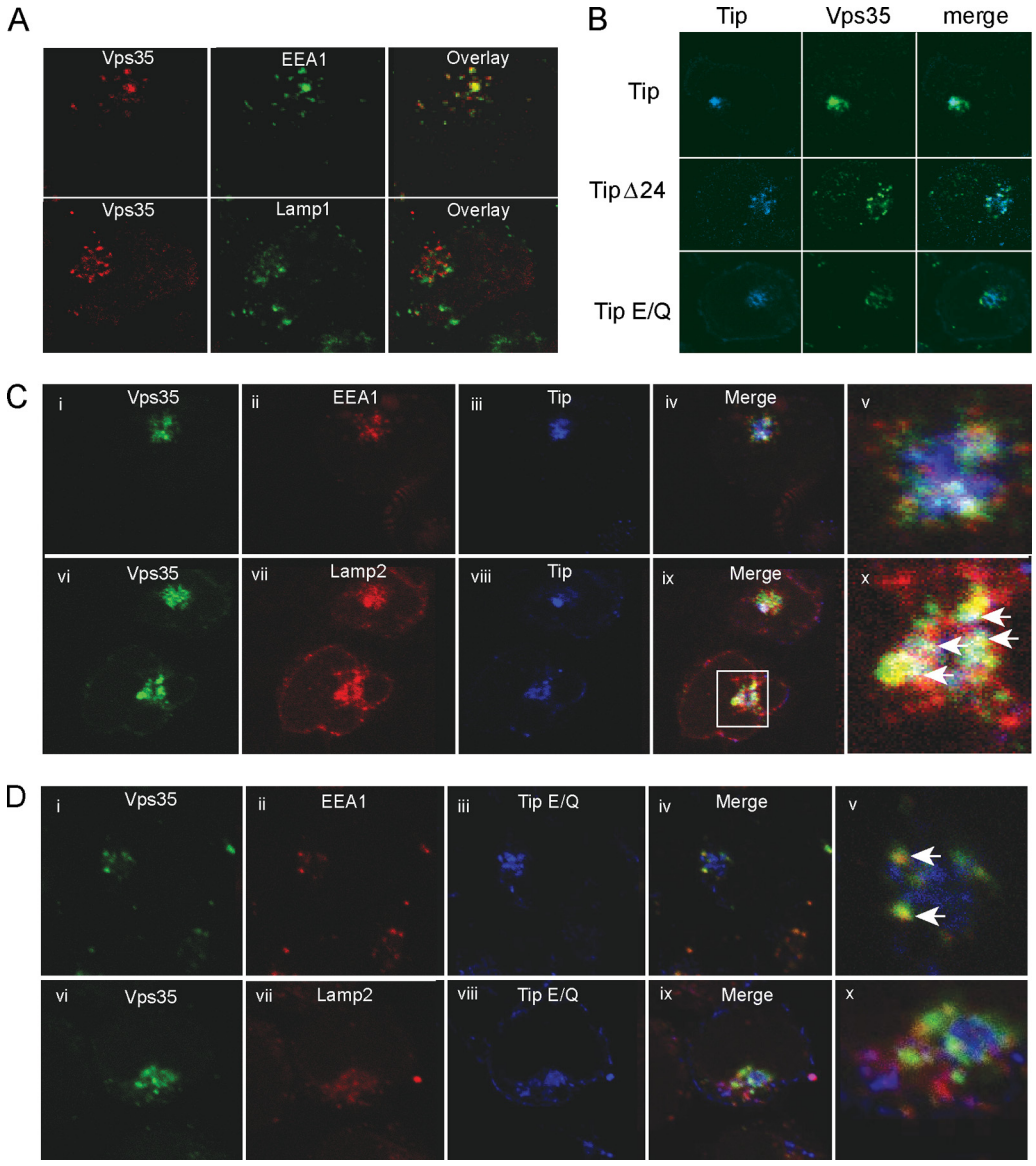

FIG. 4. Vps35 redistributes to lysosomal compartments in the presence of Tip. (A) Immunofluorescence confocal microscopy of Jurkat T cells expressing Tip or its mutants (blue) and Vps35 (green). (B) Jurkat T cells transiently expressing Vps35 (red) costained with the early endosomal marker, EEA1 (green; top), or with the lysosomal marker, Lamp1 (green; bottom). (C and D) Triple staining of Jurkat T cells for Vps35 (green), EEA1 or Lamp2 (red), and wt Tip or the Tip E/Q mutant (blue). Zoomed images of merged images from the stained cell are shown in the far right column. White arrows indicate the areas of colocalization.

5C). In addition, the expression of the Tip Δ2 p80-binding and the Tip mLBD Lck-binding mutants, both capable of binding Vps35, also detectably reduced β-glucuronidase activity (Fig. 5C). In addition, this phenotype of Tip was specific for the CI-MPR-dependent lysosomal hydrolase since the activities of the CI-MPR-independent lysosomal hydrolase, acid phosphatase, were comparable in all the tested Jurkat T cell lines. It should be noted that the decreased expression of any one of the retromer core subunits causes the other retromer core proteins to become unstable, leading to a block in efficient retromer activity (2, 44). However, Tip expression affected neither the steady-state levels of the retromer subunits Vps35, Vps26, Vps29, and SNX1 (Fig. 5D) nor their assembly (Fig. 6). Specifically, Vps35 and other retromer subunits, including Vps26 and SNX1, were copurified by the TipN42-GST fusion protein (Fig. 6A). In summary, Tip downregulates CI-MPR expression in a Vps35-binding-dependent manner, resulting in a marked reduction of CI-MPR-dependent lysosomal hydrolase enzymatic activity.

Tip interaction with Vps35 is required for CD4 downregulation. We have previously shown that expression of Tip in Jurkat T cells leads to the downregulation of CD4 on the cell surface (10, 39). Therefore, flow cytometry was performed on Jurkat T cells stably expressing the Tip Δ24 and Tip E/Q mutants to determine whether Vps35 binding to Tip had any effect on the expression of lymphocyte surface antigens. Jurkat T cells expressing the Tip Δ24 and Tip E/Q mutants had low levels of TCR expression similar to that of wt Tip. However,

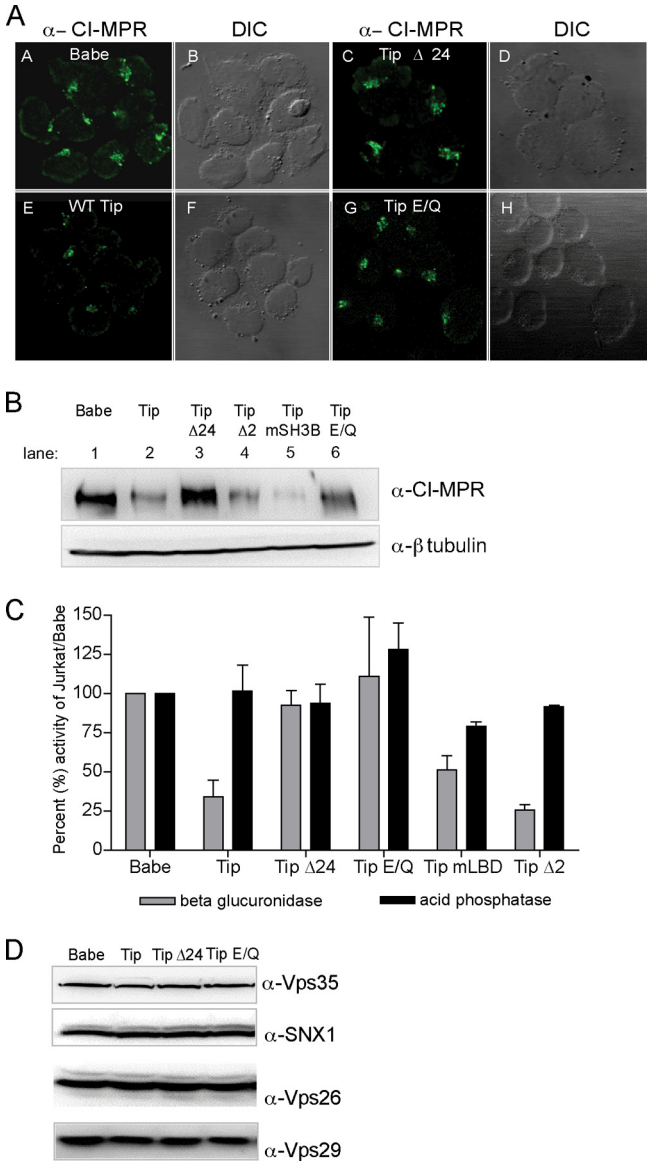

FIG. 5. Tip induces the reduction of CI-MPR levels and β-glucuronidase activity but not retromer subunit levels. Jurkat T cells stably expressing Tip and its mutants were used to determine retromer activity as assayed by CI-MPR protein levels and CI-MPR-dependent hydrolase activity. (A) Immunofluorescence confocal microscopy of endogenous CI-MPR in Jurkat stable T cell lines expressing Babe vector, Tip, or the Tip Δ24 or Tip E/Q mutant. (B) Western blot analysis of CI-MPR and β-tubulin in Jurkat stable T cells lines expressing Babe vector, Tip, Tip Δ24 mutant, Tip mSH3B, or Tip E/Q. (C) Equal amounts of protein from stably transfected Jurkat T whole-cell lysates were used to determine the activity of β-glucuronidase and acid phosphatase. Results are expressed as percent activity compared to Jurkat/Babe vector cells with means plus SD from 2 to 8 independent experiments. (D) Western blot analysis of whole-cell lysates of Jurkat stable T cell lines expressing Babe vector, Tip, or Tip Δ24 or Tip E/Q mutant, probing for steady-state levels of the endogenous retromer subunits Vps35, SNX1, Vps26, and Vps29.

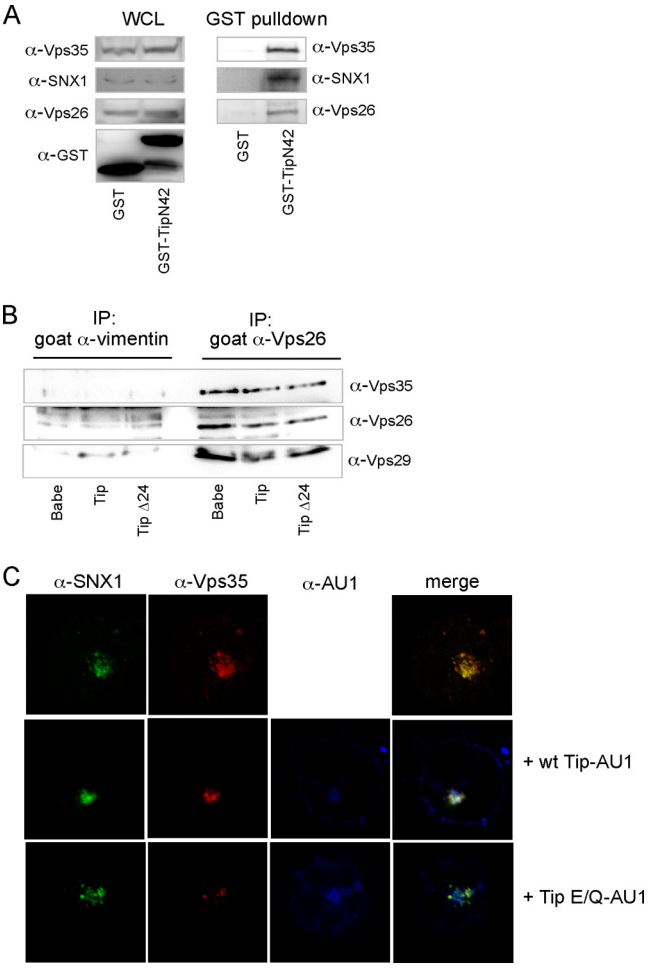

FIG. 6. Tip does not interfere with the assembly of the retromer complex. (A) Vps35-Vps26-SNX1 complex was pulled down with the N terminus of Tip. 293T cells were transfected with vectors expressing GST or TipN42-GST. GST pulldowns were performed 48 h posttransfection, followed by Western blot analysis with antibodies against Vps35, SNX1, and Vps26. (B) Vps26 and Vps29 were coimmunoprecipitated with Vps35 in the presence of Tip. Endogenous Vps26 or vimentin (control) was immunoprecipitated from cell lysates of stably transfected Jurkat T cells expressing the Babe vector, wt Tip, or the Tip Δ24 mutant, followed by Western blot analysis using antibodies against Vps35, Vps26, and Vps29. (C) SNX1 colocalized with Vps35 in the presence of wt Tip. Jurkat T cells were electroporated with vectors expressing SNX1 and Vps35 alone or with wt Tip-AU1 or Tip E/Q-AU1. Cells were prepared for immunofluorescence and confocal microscopy 48 h postelectroporation. SNX1 (green), Vps35 (red), wt Tip or Tip E/Q (blue).

they showed little or no downregulation of CD4 surface expression (Fig. 7A). As previously shown, the T cell receptor was readily downregulated on Jurkat T cells expressing wt Tip or the Tip Δ24 or Tip E/Q mutants, whereas CD45 expression was unchanged on all Jurkat T cells (Fig. 7A). Immunoblotting with anti-CD4 antibodies also showed decreased CD4 protein levels in wt Tip-expressing cells but not in Tip Δ24 cells (Fig. 7B). Quantitative real-time reverse transcription-PCR (RT-PCR) analysis of total RNAs extracted from Jurkat T cell lines showed no significant differences in the CD4 mRNA levels, suggesting that Tip downregulates CD4 expression at the post-transcriptional level (Fig. 7C). Finally, CD4 was detected on the cell surface and in intracellular compartments when transfected with a vector or the Tip Δ24 mutant. However, upon expression of wt Tip, the CD4-positive signal decreased, and

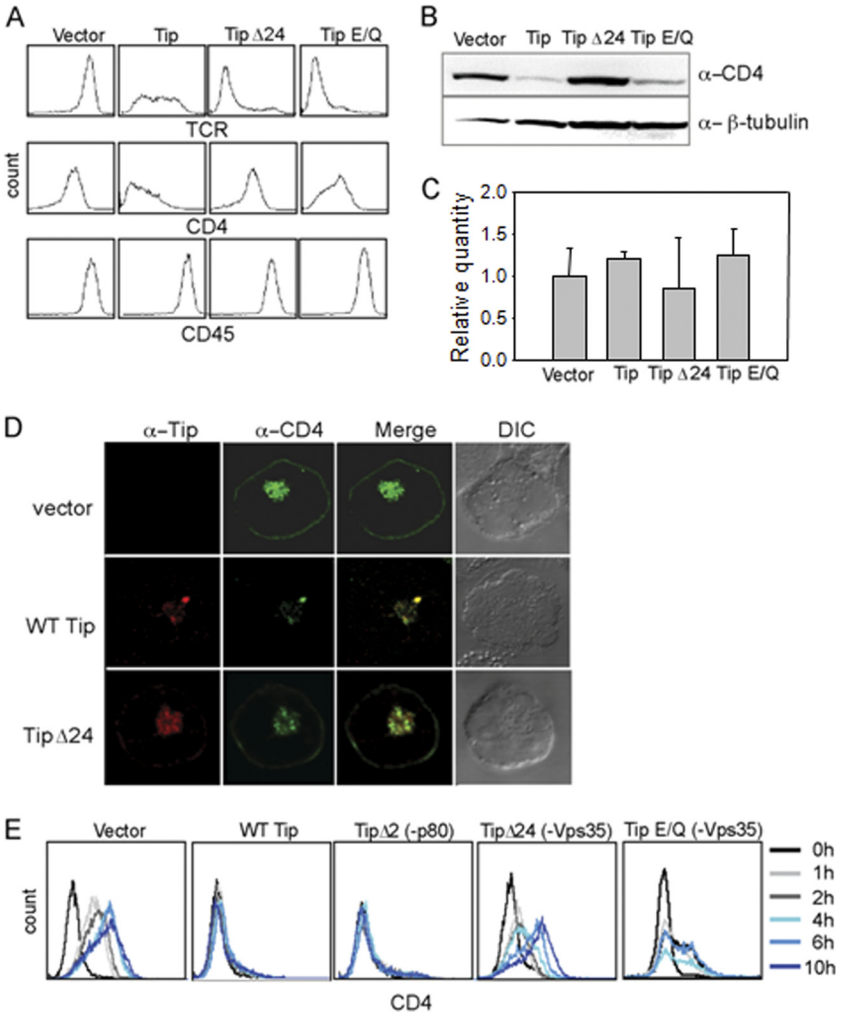

FIG. 7. Downregulation of CD4 is dependent on Tip interaction with Vps35. (A) Multicolor flow cytometric analysis of Jurkat stable T cell lines expressing vector, wt Tip, or Tip Δ24 or Tip E/Q mutant with antibodies against TCR (top), CD4 (middle), and CD45 (bottom). (B) Western blot analysis of whole-cell lysates from the indicated Jurkat stable cell lines, probing for CD4 and β-tubulin (as a loading control). (C) Quantitative real-time PCR analysis of CD4 mRNAs. For the relative quantification of CD4 mRNAs, 18S rRNA was used for normalization. (D) Confocal microscopy of Jurkat T cells transiently expressing CD4 (red) and vector (top), wt Tip (green; middle), or the Tip Δ24 mutant (green; bottom). (E) Recovery of CD4 surface expression after trypsin treatment. Jurkat stable T cell lines expressing vector, wt Tip, or Tip Δ2, Tip Δ24, or Tip E/Q mutant were treated with trypsin to remove cell surface-associated CD4, washed, and incubated at 37°C with RPMI 1640. Cells were harvested at the indicated time points and stained with anti-CD4 antibody, followed by flow cytometric analysis.

almost all of the CD4 was colocalized with Tip in intracellular compartments (Fig. 7D).

While Tip expression readily induces the downregulation of CD4 surface expression and CD4 steady-state levels in a retromer-binding manner, it was unclear how Tip mediated inhibition of CD4 expression and trafficking. To first investigate whether CD4 is able to traffic to the cell surface in the presence of Tip, the stable Jurkat T cells expressing Tip and its mutants were treated with trypsin to remove all cell surface-associated CD4, followed by incubation in regular medium without trypsin to allow newly synthesized CD4 to travel to the surface. Cells were taken at different time points after trypsin treatment and analyzed by flow cytometry for CD4 surface expression. Vector-containing cells fully recovered CD4 surface expression by 6 h after trypsin treatment, whereas cells expressing wt Tip or the Tip Δ2 mutant lacked CD4 expression on their surfaces for the duration of the experiment (Fig. 7E). Strikingly, Tip Δ24- and Tip E/Q-expressing cells showed CD4 recovery kinetics similar to those of vector-containing cells (Fig. 7E). These results comprehensively show that Tip and retromer interaction consequently affects CD4 forward trafficking, resulting in a robust downregulation of CD4 surface expression.

Tip interaction with Vps35 is required for IL-2-independent T cell immortalization. To address whether Tip interaction with Vps35 plays a role in an *in vitro* T cell immortalization, Tip 3Δ24 (deletion of amino acids 4 to 24) and Tip E/Q mutants were introduced into the HVS genome using a cosmid-based genetic manipulation approach. After transfection of the five cosmids containing wt Tip or the Tip 3Δ24 or Tip E/Q mutant into OMK permissive cells, recombinant HVS was analyzed by PCR for regions spanning the cosmids to confirm the completion of virus production and the integrity of the

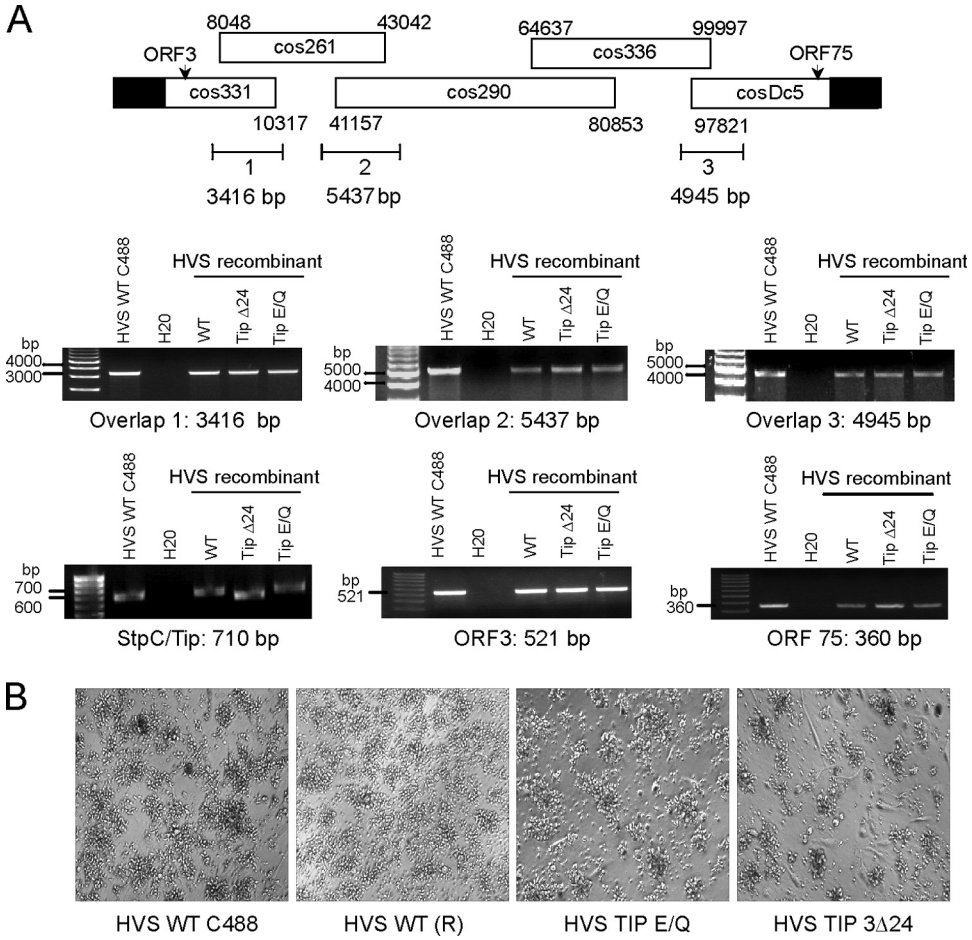

FIG. 8. Tip Vps35-binding mutant viruses can transform T cells in the absence of IL-2. (A) Schematic diagram of cosmid-based recombinant virus generation and PCR analysis of recombinant viruses used in transformation assays. HVS wt C488 (parental virus) was used as a positive control. Recombinant viruses were generated to encode wt Tip or Tip 3Δ24 or Tip E/Q mutant. PCR amplification of cosmid overlapping regions (ORF3, ORF75, and StpC/Tip) were recombined to produce full-length virus. (B) Micrographs of aggregated, transformed T cells in cultures lacking IL-2. Recombinant wt virus is denoted (R).

resulting viruses. A parental HVS C488 strain was used as a positive control. All three recombinant viruses containing wt Tip or the Tip 3Δ24 or Tip E/Q mutant were positive for each region analyzed, as well as for open reading frame 3 (ORF3)- and ORF75-encoding genes. The expected sizes of the DNA fragments containing the StpC oncogene and Tip gene were detected from all three recombinant viruses, and DNA sequence analysis showed the presence of wt Tip or the Tip 3Δ24 or Tip E/Q mutant in each virus (Fig. 8A).

Human lymphocytes isolated from healthy donors were infected with freshly isolated recombinant HVS and incubated in the absence of exogenous IL-2. Approximately 1 month after infection, most peripheral blood mononuclear cells (PBMCs) were dead, but a small population of lymphocytes started to proliferate and grew for 3 months in the absence of exogenous IL-2. Transformed cells were then split into two cultures: one part with the addition of IL-2, and the other part without. Immortalization was then defined as persistent growth for two additional months. While all four viruses were able to initially induce the aggregation and proliferation of infected lymphocytes as shown by microscopic analysis, only the parental and recombinant wt HVS were able to immortalize primary human T cells in the absence or presence of exogenous IL-2 (Fig. 8B and Table 1). In contrast, the HVS Tip E/Q or Tip 3Δ24 mutant was not able to immortalize primary human T cells to

TABLE 1. Tip Vps35-binding mutant viruses cannot immortalize T cells in the absence of exogenous IL-2[a]

Transformation or immortalization	No. of successful transformations or immortalizations/no. of attempts			
	HVS WT C488	HVS WT (R)	HVS Tip E/Q mutant	HVS Tip Δ24 mutant
Transformation (without IL-2)	6/6	6/6	6/6	6/6
Immortalization				
Without IL-2	6/6	6/6	0/6	0/6
With IL-2	6/6	6/6	0/6	1/6

[a] Summary of T cell transformation/immortalization experiments. (R) denotes recombinant wt virus.

reach permanent cell growth in the absence of exogenous IL-2 (Table 1). From six attempts, one immortalization by HVS Tip 3Δ24 was obtained under IL-2 supplementation, whereas HVS Tip E/Q-infected cells did not undergo immortalization upon any conditions (Table 1). These results suggest that Tip interaction with retromer is required for the efficient *in vitro* prolonged growth of human primary T cells.

DISCUSSION

To date, retromer has been shown to be involved primarily in the retrograde transport of CI-MPR in mammalian cells (2, 44). Recent studies have also suggested a role for retromer in IgA transcytosis and Wnt signaling, but the exact mechanisms remain unclear (12, 18, 52). Thus far, the retromer subunits have been known to be required for trafficking some known cargo proteins; HVS Tip is the first viral protein that binds to Vps35 and inhibits retromer activity. Similar to the knockdown studies of Vps26, Tip expression causes swelling of lysosomal compartments, dramatically decreases the steady-state level of CI-MPR, and reduces the activity of the CI-MPR-dependent hydrolase, β-glucuronidase (2). However, in contrast to the knockdown studies, the retromer subunits remain stable in the presence of Tip. These data suggest that Tip binding to Vps35 inhibits primarily retromer activity, possibly by blocking the exit of the retromer complex from the endosomal system since complex formation does not seem to be affected and the retromer subunits did not appear to be degraded. One proposed hypothesis is that Tip somehow blocks a regulatory step that normally allows the assembled retromer complex to exit the endosome such that the Tip-retromer complex remains associated with the endosomal compartment. Eventually, the endosome matures into a lysosome, as seen by Tip, Vps35, and Lamp2 colocalization in Fig. 3. Thus, Tip possibly tethers the assembled retromer complex to the cytoplasmic side of the endolysosomal membrane, resulting in the inhibition of retromer function.

Recently, a crystal structural analysis of the Vps35-Vps29 complex and an electron microscopy analysis of the retromer complex show that the retromer assembles into a tubelike structure at the cytoplasm-facing surface of the endosomal membrane (24). Based on this proposed assembly of the retromer, Tip proteins would most likely bind to the outer ring of this complex via Vps35. One biological consequence of the interaction between Tip and Vps35 is its effect on the forward trafficking of CD4 to the cell surface. After trypsin treatment of Jurkat T cells stably expressing Tip, little or no CD4 reaches to the cell surface, suggesting that Tip immediately redirects newly synthesized CD4 for degradation. While it is possible that CD4 traffics to the surface of Tip-expressing cells and then is quickly endocytosed, this is not a likely scenario since nearly no positive CD4 staining was detected at any of the tested time points. Similar CD4 recovery kinetics on the cell surface was also seen when lipid rafts were disrupted with Filipin III treatment (10). In addition, the carboxyl-terminal transmembrane of Tip is required for its lipid raft localization (10) and oligomerization (33), as well as for the efficient downregulation of CD4 surface expression. Thus, the lipid raft localization and oligomerization of Tip may facilitate the lysosomal trafficking of associated cellular proteins, including the retromer complex from endosomal compartments (33). Although the precise roles of lipid rafts for retromer function have yet to be determined, phosphatidylinositol lipids have been shown to directly contribute to the membrane recruitment of sorting nexins (26) and the distribution of retromer components and retrograde sorting (15, 42). Furthermore, the effect of Tip-mediated inhibition of retromer function seems to be specific for CD4 trafficking, as CD45 surface expression and transferrin receptor endocytosis were unaffected in Tip-expressing cells (unpublished results). It is interesting to note that retromer complexes not only mediate retrograde trafficking between endosomes to the trans-Golgi network but also direct endosome-to-plasma membrane traffic of β2 adrenergic receptor (51). Further studies are needed to determine the precise mechanism by which Tip inhibits CD4 trafficking to the cell surface through the interaction with the retromer complex. While many lymphotropic viruses employ CD4 downregulation as part of their evasive strategies (1, 3, 8, 32, 40, 46), HVS utilizes a unique mechanism to lower CD4 expression at the cell surface, which may consequently allow for decreased immune surveillance of infected cells *in vivo*.

Along with the Stp-C oncogene, Tip expression is required for HVS-induced T cell immortalization. Stp-C is known to activate NF-κB through its association with tumor necrosis factor (TNF) receptor-associated factor (TRAF) proteins, which leads to the signaling necessary for T cell transformation (30). However, the mechanism by which Tip contributes to T cell transformation remains elusive. Tip interaction with Vps35 may be a potential mechanism that contributes to HVS-induced T cell transformation given that Tip effectively inhibits retromer activity and Tip expression leads to swollen lysosomal compartments, a characteristic that has also been described in some cancer-derived cells (28). In addition, many cancerous cells have abnormal lysosomal hydrolase trafficking activities that aid in cancer growth. Furthermore, because the loss of CI-MPR expression is an early event in many cancers, it has been implicated as a tumor suppressor (19).

In order to study whether retromer targeting by Tip contributes to HVS-induced T cell immortalization, mutant viruses were generated with a Tip mutant that no longer interacts with Vps35. Unlike wild-type HVS, neither the HVS Tip E/Q nor the HVS Tip Δ24 mutant is able to immortalize primary T cells in the absence of IL-2, and out of six attempts in the presence of IL-2, only one immortalized T cell line was obtained with HVS Tip Δ24. While signaling from Tip interactions with p80 and Lck may contribute to transformation, the inhibition of retromer function by Tip is required for the complete immortalization of primary T cells. One possible explanation that links the inhibition of retromer activity by Tip and the suppression of immortalization is the downregulation of CI-MPR, which has been implicated in numerous regulatory and transport functions and is suggested to be a tumor suppressor protein (27). Several features of CI-MPR may support this notion. First, CI-MPR is frequently mutated in human breast and colon cancers (5). Second, the abnormal regulation of CI-MPR-mediated trafficking of lysosomal hydrolase enzymes is linked to aberrant cell growth. For example, lysosomal cysteine cathepsins are highly upregulated in a wide variety of cancers by mechanisms ranging from gene amplification to posttranscriptional modification (34). Finally, CI-MPR is the receptor

of granzyme B, a serine protease released into targeted cells by cytotoxic T lymphocytes (35). Conceivably, granzyme B interacts with CI-MPR to block the excessive release of lysosomal enzymes that induce cell death. Besides the downregulation of CI-MPR, Tip-mediated downregulation of CD4 surface expression may be directly or indirectly involved in HVS transformation. A previous study has shown that the ligation of CD4 with anti-CD4-specific antibodies or gp120 from human immunodeficiency virus inhibits the growth of HVS-transformed T cells and that this can be reversed by the addition of exogenous IL-2 (6). In fact, a similar phenotype is seen in the HVS Tip Δ24-transformed T cells, wherein T cell immortalization is possible only upon IL-2 supplementation. This indicates that HVS evolved to acquire the Tip gene in order to deregulate host retromer function and ultimately deregulate CI-MPR activity and CD4 function, which may contribute to HVS-induced pathogenesis. However, given that retromer is conserved from yeast to mammals, it is also very likely that retromer may be involved in other cellular functions, which have yet to be uncovered. Nevertheless, we demonstrate that a herpesvirus protein specifically targets Vps35 and reduces retromer activity, contributing to a dramatic decrease in CI-MPR and CD4 surface expression and ultimately leading to HVS-induced T cell immortalization.

ACKNOWLEDGMENTS

This work was partly supported by U.S. Public Health Service grants CA31363, CA109697, AI073099, and RR00168, by Hastings Foundation and Fletcher Jones Foundation grants (to Jae Ung Jung), and by the National Research Foundation of Korea (NRF) grants (2009-0070600 and 2010-0019472) funded by the South Korean government (MEST) to Nam-Hyuk Cho.

The funders had no role in study design, data collection and analysis, decision to publish, or preparation of the manuscript.

We thank D. Baumjohann and M. Neagu for their critical reading of the manuscript.

REFERENCES

1. **Aiken, C., J. Konner, N. R. Landau, M. E. Lenburg, and D. Trono.** 1994. Nef induces CD4 endocytosis: requirement for a critical dileucine motif in the membrane-proximal CD4 cytoplasmic domain. Cell **76:**853–864.
2. **Arighi, C. N., L. M. Hartnell, R. C. Aguilar, C. R. Haft, and J. S. Bonifacino.** 2004. Role of the mammalian retromer in sorting of the cation-independent mannose 6-phosphate receptor. J. Cell Biol. **165:**123–133.
3. **Barry, M., S. F. Lee, L. Boshkov, and G. McFadden.** 1995. Myxoma virus induces extensive CD4 downregulation and dissociation of p56lck in infected rabbit CD4+ T lymphocytes. J. Virol. **69:**5243–5251.
4. **Biesinger, B., et al.** 1995. The product of the *Herpesvirus saimiri* open reading frame 1 (tip) interacts with T cell-specific kinase p56lck in transformed cells. J. Biol. Chem. **270:**4729–4734.
5. **Braulke, T., L. Mach, B. Hoflack, and J. Glossl.** 1992. Biosynthesis and endocytosis of lysosomal enzymes in human colon carcinoma SW 1116 cells: impaired internalization of plasma membrane-associated cation-independent mannose 6-phosphate receptor. Arch. Biochem. Biophys. **298:**176–181.
6. **Broker, B. M., et al.** 1994. Engagement of the CD4 receptor inhibits the interleukin-2-dependent proliferation of human T cells transformed by *Herpesvirus saimiri*. Eur. J. Immunol. **24:**843–850.
7. **Carlton, J., et al.** 2004. Sorting nexin-1 mediates tubular endosome-to-TGN transport through coincidence sensing of high-curvature membranes and 3-phosphoinositides. Curr. Biol. **14:**1791–1800.
8. **Chen, B. K., R. T. Gandhi, and D. Baltimore.** 1996. CD4 down-modulation during infection of human T cells with human immunodeficiency virus type 1 involves independent activities of *vpu*, *env*, and *nef*. J. Virol. **70:**6044–6053.
9. **Cho, N. H., et al.** 2004. Inhibition of T cell receptor signal transduction by tyrosine kinase-interacting protein of *Herpesvirus saimiri*. J. Exp. Med. **200:**681–687.
10. **Cho, N. H., et al.** 2006. Association of herpesvirus saimiri tip with lipid raft is essential for downregulation of T-cell receptor and CD4 coreceptor. J. Virol. **80:**108–118.
11. **Collins, B. M., C. F. Skinner, P. J. Watson, M. N. Seaman, and D. J. Owen.** 2005. Vps29 has a phosphoesterase fold that acts as a protein interaction scaffold for retromer assembly. Nat. Struct. Mol. Biol. **12:**594–602.
12. **Coudreuse, D. Y., G. Roel, M. C. Betist, O. Destree, and H. C. Korswagen.** 2006. Wnt gradient formation requires retromer function in Wnt-producing cells. Science **312:**921–924.
13. **Duboise, S. M., J. Guo, S. Czajak, R. C. Desrosiers, and J. U. Jung.** 1998. STP and Tip are essential for herpesvirus saimiri oncogenicity. J. Virol. **72:**1308–1313.
14. **Edgar, A. J., and J. M. Polak.** 2000. Human homologues of yeast vacuolar protein sorting 29 and 35. Biochem. Biophys. Res. Commun. **277:**622–630.
15. **Falguieres, T., et al.** 2001. Targeting of Shiga toxin B-subunit to retrograde transport route in association with detergent-resistant membranes. Mol. Biol. Cell **12:**2453–2468.
16. **Fickenscher, H., and B. Fleckenstein.** 2001. Herpesvirus saimiri. Philos. Trans. R. Soc. Lond. B Biol. Sci. **356:**545–567.
17. **Franch-Marro, X., et al.** 2008. Wingless secretion requires endosome-to-Golgi retrieval of Wntless/Evi/Sprinter by the retromer complex. Nat. Cell Biol. **10:**170–177.
18. **George, A., H. Leahy, J. Zhou, and P. J. Morin.** 2007. The vacuolar-ATPase inhibitor bafilomycin and mutant VPS35 inhibit canonical Wnt signaling. Neurobiol. Dis. **26:**125–133.
19. **Ghosh, P., N. M. Dahms, and S. Kornfeld.** 2003. Mannose 6-phosphate receptors: new twists in the tale. Nat. Rev. Mol. Cell Biol. **4:**202–212.
20. **Haft, C. R., et al.** 2000. Human orthologs of yeast vacuolar protein sorting proteins Vps26, 29, and 35: assembly into multimeric complexes. Mol. Biol. Cell **11:**4105–4116.
21. **He, X., F. Li, W. P. Chang, and J. Tang.** 2005. GGA proteins mediate the recycling pathway of memapsin 2 (BACE). J. Biol. Chem. **280:**11696–11703.
22. **Heck, E., et al.** 2006. Growth transformation of human T cells by herpesvirus saimiri requires multiple Tip-Lck interaction motifs. J. Virol. **80:**9934–9942.
23. **Heck, E., et al.** 2005. T-cell growth transformation by herpesvirus saimiri is independent of STAT3 activation. J. Virol. **79:**5713–5720.
24. **Hierro, A., et al.** 2007. Functional architecture of the retromer cargo-recognition complex. Nature **449:**1063–1067.
25. **Horazdovsky, B. F., et al.** 1997. A sorting nexin-1 homologue, Vps5p, forms a complex with Vps17p and is required for recycling the vacuolar protein-sorting receptor. Mol. Biol. Cell **8:**1529–1541.
26. **Johannes, L., and C. Wunder.** 2011. Retrograde transport: two (or more) roads diverged in an endosomal tree? Traffic **12:**956–962.
27. **Klumperman, J., et al.** 1993. Differences in the endosomal distributions of the two mannose 6-phosphate receptors. J. Cell Biol. **121:**997–1010.
28. **Kroemer, G., and M. Jaattela.** 2005. Lysosomes and autophagy in cell death control. Nat. Rev. Cancer **5:**886–897.
29. **Kurten, R. C., et al.** 2001. Self-assembly and binding of a sorting nexin to sorting endosomes. J. Cell Sci. **114:**1743–1756.
30. **Lee, H., et al.** 1999. Role of cellular tumor necrosis factor receptor-associated factors in NF-kappaB activation and lymphocyte transformation by herpesvirus saimiri STP. J. Virol. **73:**3913–3919.
31. **Lund, T. C., R. Garcia, M. M. Medveczky, R. Jove, and P. G. Medveczky.** 1997. Activation of STAT transcription factors by herpesvirus saimiri Tip-484 requires p56lck. J. Virol. **71:**6677–6682.
32. **Mansouri, M., et al.** 2003. The PHD/LAP-domain protein M153R of myxomavirus is a ubiquitin ligase that induces the rapid internalization and lysosomal destruction of CD4. J. Virol. **77:**1427–1440.
33. **Min, C. K., et al.** 2008. Role of amphipathic helix of a herpesviral protein in membrane deformation and T cell receptor downregulation. PLoS Pathog. **4:**e1000209.
34. **Mohamed, M. M., and B. F. Sloane.** 2006. Cysteine cathepsins: multifunctional enzymes in cancer. Nat. Rev. Cancer **6:**764–775.
35. **Motyka, B., et al.** 2000. Mannose 6-phosphate/insulin-like growth factor II receptor is a death receptor for granzyme B during cytotoxic T cell-induced apoptosis. Cell **103:**491–500.
36. **Nothwehr, S. F., P. Bruinsma, and L. A. Strawn.** 1999. Distinct domains within Vps35p mediate the retrieval of two different cargo proteins from the yeast prevacuolar/endosomal compartment. Mol. Biol. Cell **10:**875–890.
37. **Nothwehr, S. F., S. A. Ha, and P. Bruinsma.** 2000. Sorting of yeast membrane proteins into an endosome-to-Golgi pathway involves direct interaction of their cytosolic domains with Vps35p. J. Cell Biol. **151:**297–310.
38. **Park, J., et al.** 2003. Distinct roles of cellular Lck and p80 proteins in herpesvirus saimiri Tip function on lipid rafts. J. Virol. **77:**9041–9051.
39. **Park, J., et al.** 2002. Herpesviral protein targets a cellular WD repeat endosomal protein to downregulate T lymphocyte receptor expression. Immunity **17:**221–233.
40. **Piguet, V., et al.** 1998. Mechanism of Nef-induced CD4 endocytosis: Nef connects CD4 with the mu chain of adaptor complexes. EMBO J. **17:**2472–2481.
41. **Port, F., et al.** 2008. Wingless secretion promotes and requires retromer-dependent cycling of Wntless. Nat. Cell Biol. **10:**178–185.
42. **Raa, H., et al.** 2009. Glycosphingolipid requirements for endosome-to-Golgi transport of Shiga toxin. Traffic **10:**868–882.
43. **Reddy, J. V., and M. N. Seaman.** 2001. Vps26p, a component of retromer, directs the interactions of Vps35p in endosome-to-Golgi retrieval. Mol. Biol. Cell **12:**3242–3256.

44. **Seaman, M. N.** 2004. Cargo-selective endosomal sorting for retrieval to the Golgi requires retromer. J. Cell Biol. **165:**111–122.
45. **Seaman, M. N., and H. P. Williams.** 2002. Identification of the functional domains of yeast sorting nexins Vps5p and Vps17p. Mol. Biol. Cell **13:**2826–2840.
46. **Secchiero, P., et al.** 1997. Human herpesvirus 7 induces the down-regulation of CD4 antigen in lymphoid T cells without affecting p56lck levels. J. Immunol. **159:**3412–3423.
47. **Shi, H., R. Rojas, J. S. Bonifacino, and J. H. Hurley.** 2006. The retromer subunit Vps26 has an arrestin fold and binds Vps35 through its C-terminal domain. Nat. Struct. Mol. Biol. **13:**540–548.
48. **Sleat, D. E., and P. Lobel.** 1997. Ligand binding specificities of the two mannose 6-phosphate receptors. J. Biol. Chem. **272:**731–738.
49. **Small, S. A., et al.** 2005. Model-guided microarray implicates the retromer complex in Alzheimer's disease. Ann. Neurol. **58:**909–919.
50. **Sohar, I., D. Sleat, C. Gong Liu, T. Ludwig, and P. Lobel.** 1998. Mouse mutants lacking the cation-independent mannose 6-phosphate/insulin-like growth factor II receptor are impaired in lysosomal enzyme transport: comparison of cation-independent and cation-dependent mannose 6-phosphate receptor-deficient mice. Biochem. J. **330**(Pt. 2)**:**903–908.
51. **Temkin, P., et al.** 2011. SNX27 mediates retromer tubule entry and endosome-to-plasma membrane trafficking of signalling receptors. Nat. Cell Biol. **13:**715–721.
52. **Verges, M., et al.** 2004. The mammalian retromer regulates transcytosis of the polymeric immunoglobulin receptor. Nat. Cell Biol. **6:**763–769.
53. **Wieser, C., et al.** 2005. Regulated and constitutive expression of anti-inflammatory cytokines by nontransforming herpesvirus saimiri vectors. Gene Ther. **12:**395–406.
54. **Zhong, Q., et al.** 2002. Endosomal localization and function of sorting nexin 1. Proc. Natl. Acad. Sci. U. S. A. **99:**6767–6772.